

Detection of Lung Boundary in Chest X-rays using Adaptive Lung Atlas and Graph Cuts

Jeevitha Sivasamy¹, Dr. T.S. Subashini²

¹Ph.D., Scholar, Dept.of Computer and Information Science, Annamalai University, Annamalai Nagar, Tamilnadu, India.

²Associate Professor, Department of Computer Science & Engg., Annamalai University, Annamalai Nagar, Tamilnadu, India

ABSTRACT

In contrast to film X-rays the advent of digital X-rays has led to the use of computer assisted systems to automatically detect and diagnose diseases. Though CT and MRI are known for its diagnostic superiority Chest X-rays still remains the mainstay of chest imaging and is widely used by doctors to access various chest related ailments which includes pathologies related to lungs, esophagus, blood vessel, diaphragm, trachea, bronchia etc. The applicability of any computer aided diagnosis system (CAD) mainly depends on the accurate segmentation of the region of interest (ROI). In this work we have attempted to accurately segment the lung boundary using atlas based methods and non-rigid registration of atlases to patient specific adaptive lung models. The proposed work first applies a content based retrieval approach to select similar X-rays (lung masks) to that of the test X-ray using similarity measures and then an atlas of the test lung is obtained by SIFT-flow registration of the test X-ray with that of the retrieved masks. Finally graph-cut optimization is applied to extract the exact lung boundary.

Keywords : CAD, Content Based Image Retrieval, Image Registration, Radon Transform, SIFT-Flow, Graph cut segmentation.

I. INTRODUCTION

Doctors widely use chest X-ray as a means for evaluating various lung diseases like asthma, pneumonia, tuberculosis (TB) etc. Today technological innovations has led to the invention of various invasive medical imaging modalities for analysis of lung diseases, however the doctors solely depend on chest X-rays as it is easily acquirable and cheap. Today digital chest X-ray imaging, where digital X-rays are replacing traditional film based X-rays and Fig. 1 shows the digital chest X-ray.

The quality of digital chest radiography is far better compared to film X-rays and also the storage, retrieval

of digital X-ray is easy. Also digital chest X-rays has facilitated the application of computer vision techniques to automatically segment, detect and diagnose various chest related ailments.



Fig. 1 Digital Chest X-ray

The availability chest X-ray in digital format has led researchers to develop computer based systems that

could automatically segment the lung region and aid the physician in disease detection and diagnosis.

Segmentation of lung region in chest X-rays is the prerequisite to diagnosis and to assess the extent of various lung diseases. This proposed work deals with automatic lung segmentation from digital chest X-rays. Lung region segmentation is not an easy process due to un-defined and un-clear boundary between regions, low contrast, other artifacts and noise. Traditional segmentation methods based on local threshold, region growing or edge detection fails to delineate the lung boundary accurately and so more powerful strategies are required. Accurate segmentation of the lung region is very essential because subsequent image analysis solely depends on it. For this, prior knowledge about the lung region to be segmented can be incorporated into the segmented process and in this work a deformable lung atlas model is employed into the system to improve the segmentation process.

II. Literature Review

This section discusses the research work seen in the literature on chest X-ray segmentation. Segmentation methods for CXR seen in the literature include rule based scheme, thresholding(local), edge detection, ridge detection, region growing, morphological operations, and geometrical models.

The efficacy of any CAD system for lung disease depends on accurate segmentation of the lung boundary. This section reviews literature related to works on lung segmentation. There has been considerable effort applied in the development of automated lung segmentation methods and a survey is given in [1]. Pixel classification-based include thresholding, edge detection and feature based pixel classification methods. The authors in [2] constructed the statistical model of the lung using a large database. Shape information and other region feature such as centroid, eccentricity etc., were employed. The proper threshold value is computed by optimization via

iterative process. The Mahalanobis distance is used as the similarity metric to compare the statistical model created with that of the test image.

A heuristic edge-tracing approach was employed in [3] and the authors validated their results with lung contours manually drawn by experts. The authors in [4] used pixel based features to classify the various anatomical parts such as heart, lung and axilla. However this method fails to provide a high-level representation of the image content. In [5] the lungs are segmented using Connected Component Labeling and thresholding. The Airways are segmented using region growing technique and eliminated from the segmented lung region. Then morphological opening and closing are used for smoothing to remove noise. A combination of global and local thresholding was employed in [6] followed by contour smoothing to segment the lung region. Bidirectional chain coding method combined with a support vector machine (SVM) classifier is used to selectively smooth the lung border while minimizing the over segmentation of adjacent regions in [7]. To reduce over-segmentation, an improved watershed segmentation algorithm is proposed by the authors in [8] to segment and extract lung parenchyma.

Machine learning based methods such as support vector machine, random forest, neural network using intensity, texture shape and neighbouring anatomical features of the lung was proposed in [9] and [10] to segment the lung region. However correct classification depends on the most relevant and discriminant features. Non-negative matrix factorization (NMF) was proposed in [11] where the spatial interaction of the neighbouring voxel and K-means clustering was applied to segment the lung voxel from the CT image. Active contour modeling is employed in [12] to segment lung with pathologies. The concept of the Fully Convolutional Net for a pixel wise classification to segment lung region with a nonlinear, local-to-global feature representation is introduced in [13]. Authors in [14] performed lung segmentation based on atlas registration and SIFT-

flow methods which can segment lung including all kinds of pathological changes. Statistical deformation model such as ASM [15] are widely seen in literature for lung segmentation in CRXs and CT lung images.

Making use specific lung models created using similar chest X-ray images related to the patient chest X-ray, this work presents a method using SIFT-Flow non-rigid registration technique and graph cut segmentation technique to accurately detect lung boundaries in chest X-rays.

III. Proposed Methodology with Experimental Results

In this work to segment the lung region in CXR, content based retrieval approach will be first applied to select similar X-rays (lung masks) to that of the test X-ray using similarity measures and then an atlas of the test lung will be created using SIFT-flow registration. Finally graph-cut optimization will be applied to extract the exact lung boundary. The proposed method was tested with the publicly available JSRT database. The overall block diagram of the proposed method is shown in Fig. 2. The entire work is divided into 3 major modules namely A. CBIR Framework, B. Creation of Lung atlas and C. Segmentation of Lung region.

A. CBIR Framework

Since the JSRT database contains CXRs which have variable lung shapes, it is not possible to use a single static model of the lung for segmentation. So, as the first step to in order to create the adaptive lung model a CBIR framework using Radon transform and Bhattacharya distance metric is employed to retrieve top four similar images which are then used in the next module to create an accurate lung model using SIFT- Flow based on-rigid registration method.

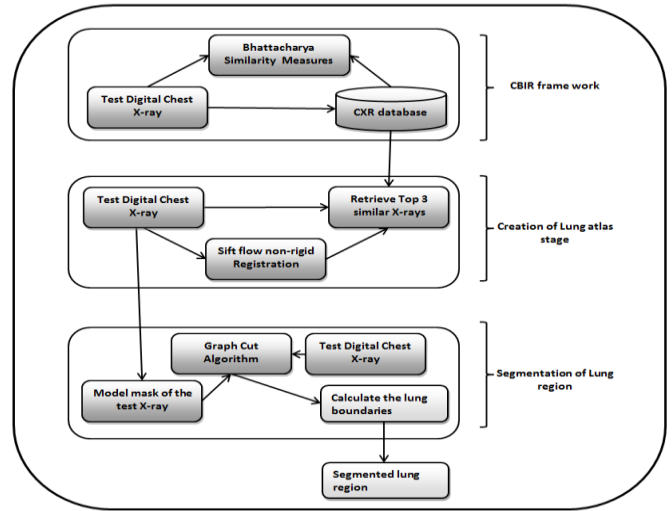


Fig. 2 Block diagram of the proposed lung segmentation method

Radon transform [16] is applied to all the images in JSRT database to calculate the intensity projection of the histogram-equalized images in the vertical and the horizontal directions. The Radon transform of an image is defined mathematically as:

$$R(x', \theta) = \iint_{-\infty}^{\infty} f(x, y) \delta(x \cos \theta + y \sin \theta - x') dx dy$$

Radon transform $R(x', \theta)$ of an image $f(x, y)$ can be defined as a series of line integrals through $f(x, y)$ at different offsets from the origin and this is shown in Fig. 3. The Radon transform takes a projection of a 2D image along a direction to give the 1D profile. This helps to speed up the retrieval process. Where θ the angle of the line and x' is the perpendicular offset of the line and $\delta(\cdot)$ is the 2-D impulse function. The Radon transform computes a projection of the image as a sum of line integrals accumulating pixel intensities along rays defined by $x' = x \cos \theta + y \sin \theta$ in the x - y plane.

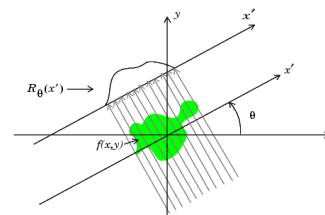


Fig. 3 Radon Transform

Then we measure the similarity of each projection profile between the atlas database and the patient chest X-ray using the average **Bhattacharyya coefficient** [17] which is given by:

$$Bhatt_{coeff}(Img_1, Img_2) = \gamma \sum_{a=1}^p \sqrt{m_1(a)m_2(a)} + (1 - \gamma) \sum_{b=1}^q \sqrt{n_1(b)n_2(b)}$$

Where $m_1(a)$ and $m_2(a)$ are the horizontal projections, $n_1(b)$ and $n_2(b)$ are the vertical projections of images Img_1 and Img_2 , respectively, a and b are the histogram bins of the projections profiles, p and q are the number of bins in the profile histograms, and $\gamma = p/(p+q)$ is the relative weight for each profile; when $p=q, \gamma = 1/2$. Fig. 4 shows the top four similar images retrieved after the application of proposed CBIR framework and in Fig. 4(a) the test image itself is retrieved as the top most similar image.

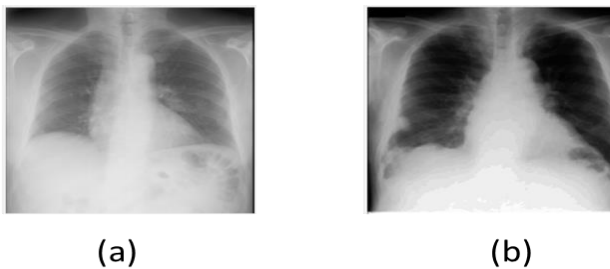


Fig. 4 (A) Test X-Ray Figs. 4 (B), 4 (C), 4 (D) Top Four (Excluding The Original Image) Three Similar Images Retrieved After The Application Of Proposed CBIR Framework.

B. Creation of Lung Atlas

Lung region in CXR images can vary significantly across patients due to different shapes and sizes. Therefore, accounting for this variability is crucial for proper segmentation and for this one or more atlases are used to represent the lung region. An atlas refers to a specific model of the image under investigation with parameters that are learned from the top four similar lung images retrieved in the earlier step. Using these learned parameters, the statistical model of the

lung under investigation is created by a non-rigid image SIFT-flow image registration algorithm. The process that tries to align one or more images is referred to as image registration, where one image is taken as the source and the other the target. In this work, for creating the lung atlas, instead of considering all the images in the database for registration, only top four images that best resemble the patient test image are considered. This helps to speed up the registration process in contrast to considering all images present in the database.

This work employs SIFT flow algorithm for creating the lung atlas. The SIFT flow algorithm [18] works as follows. A 16x16 neighborhood of every pixel in an image is divided into a 4 x 4 cell array. Then the orientation of each cell array is quantized into 8 bins resulting in a 4 x 4 x 8 = 128 dimensional SIFT descriptor per pixel. A pair of SIFT images (s_1, s_2) are matched using an **objective function** $E(w)$ on SIFT descriptors. The minimization algorithm calculates the SIFT-flow w by minimizing the objective function

$$E(w) = \sum_p \min(\|s_1(p) - s_2(p + w(p))\|_1, t) + \sum_p \eta (|u(p)| + |v(p)|) + \sum_{(p,q) \in \epsilon} (\min(\alpha |u(p)| - |u(q)|, d) \min(\alpha |v(p)| - |v(q)|, d))$$

$E(w)$ consists of 3 terms, the *data term* which constrains to match the SIFT descriptor at the image position $p = (x, y)$ via the flow vector $w(p) = (u(p), v(p))$, the *small displacement term* constrains the flow vectors to be as small as possible, and the *smoothness term* which constrains the adjacent pixels to have similar displacement.

Fig. 5 illustrates the registration stage of the proposed system. Fig. 5(a) is the patient X-ray. Fig. 5(b), (c), (d) are the most similar X-ray to the patient X-ray in the database chosen according to the shape similarity between the lungs. The SIFT-flow algorithm calculates corresponding matches for each pixel of these X-ray pair by solving the flow vectors. The spatial shifts between corresponding matches define the

transformation mapping forpixels. The algorithm applies the transformation mapping by simply shifting each pixel in the training mask according to the calculated shift distance. The registration stage is repeated for each of the top-4 (e.g.,) similar X-rays to the patient X-ray.

The lung model for the patient X-ray is built-up using the mean of the top-ranked registered masks. The computed patient specific lung model is shown in fig. 5(e). Since the SIFT-flow method applies the transformation mapping for each pixel independently, the registered masks forming the lung atlas model have rough boundaries and subsequently cubic spline interpolation [57] is applied to the lung mask to obtain smooth boundaries.

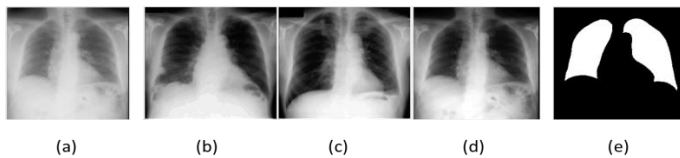


Fig. 5(A) Is The Patient Test X-Ray (B), (C), (D) are the Most Similar X-Ray to the Patient X-Ray in the Database Chosen According to the Shape Similarity Between The Lungs, (E) Averaged Patient Specific Lung Model

C. Segmentation of Lung Region

Using the characteristics of the lung mask obtained in the previous step this module detects lung boundary of X-ray images using graph cut technique [19]. This technique converts an image into a graph, where each pixel is connected to its neighboring nodes by weighted edges as well as terminal nodes namely source (foreground) and sink (background). The higher the probability that pixels are related to its neighbours or the terminal nodes the higher is the edge weight. The edge weights determine whether a pixel is likely to be foreground or background and whether a pixel is likely to have same label as neighbors. The algorithm cuts along weak edges, achieving the segmentation of objects in the image

and weight of cut is the sum of the weight of edges removed. Fig. 6 shows the basic idea of Graph cuts.

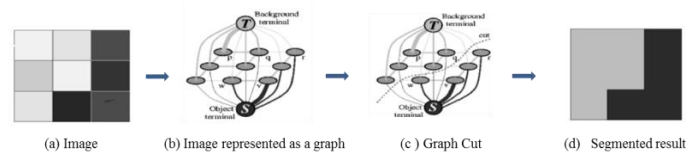


Fig. 6 Graph cut Segmentation (a) Shows image to be segmented, (b) Graph showing all the nodes connected to Source and Sink Nodes, (c) Graph cut cuts along weak edges so there is no path from source to sink, (d) Segmented image

Graph cut algorithm seeks division of image into foreground and background with the help an objective function given in the equation below.

$$E(f) = \alpha_1 E_d(f) + \alpha_2 E_s(f) + \alpha_3 E_m(f)$$

where $E_d(f)$ is the data term, $E_s(f)$ is the smoothness term and $E_m(f)$ represent the lung model. To minimize this objective function max-flow-min-cut algorithm [20] is used which partitions the graph into two sub-graphs. This connects a pixel to either to the source node or sink node and thus labeling the pixels in the image as either foreground or background pixels

The lung segmentation results are shown in Fig. 7, where Fig. 7(a) is the patient X-ray. Fig. 7(b), (c), (d) are the top three images retrieved from the database using the proposed CBIR framework elaborated in section II.C. Fig 7(e) shows the lung mask generated using SIFT-Flow registration technique. Using the lung mask generated the detected lung boundary is shown in Fig. 7 (f).

The experiments were carried out using the chest images available in the JSRT (Japanese Society of Radiological Technology) dataset. The data set contains totally 247 chest X-rays whose size is 2048 x 2048 pixels and uses 12 bits to represent the gray-scale intensity. Fig 8 shows results of the proposed work on other two randomly chosen X-rays of the JSRT database.

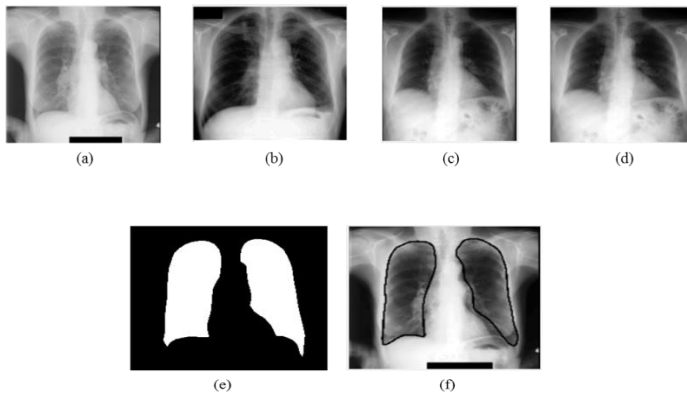


Fig. 7 Segmentation Results (a)Patient chest X-ray. 7(b), (c), (d) are the most similar X-ray to the patient X-ray in the database chosen according to the shape similarity between the lungs. 7(e) Averaged patient specific lung model 7(f) Segmented lung boundary

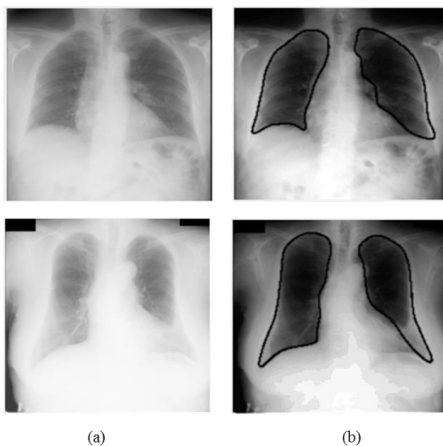


Fig. 8 Segmentation Results (a) Patient Chest X-ray, (b) Segmented lung boundary

IV. Conclusion

A method to detect lung boundary from chest X-rays using lung specific model and graph cut technique was proposed in this work. As the first step, Radon transform is used to extract the horizontal and vertical projection profiles of each image and Bhattacharyya coefficient is used as the similarity metric to retrieve the top four X-ray images from the database that best resembles the X-ray under investigation. Then an atlas of the test lung is obtained by SIFT-flow registration

of the test X-ray with that of the retrieved masks. Finally graph-cut optimization is applied to extract the exact lung boundary. Subjective evaluation of the segmentation results with the Radiologist of Rajah Muthiah Medical College Hospital, Annamalainagar indicates that the results are promising and could be employed to automatically detect lung boundaries from chest X-ray Images.

V. Acknowledgement

The authors would like to thank Dr. M.K. Sivakkolunthu, Professor of Radiology, Raja Muthiah Medical College Hospital, Annamalai Nagar for his valuable help and comments in carrying out this work.

VI. References

- [1] B. Ginneken, Bart M terHaarRomeny, and Max A Viergever. *Computer-aided diagnosis in chest radiography: a survey*. IEEE TMI, 20(12):1228–1241, 2001.
- [2] A. Dawoud, "Lung segmentation in chest radiographs by fusing shape information in iterative thresholding", IET Comput. Vision, Vol. 5, Iss. 3, pp. 185–190, 2011.
- [3] Duryea J, Boone JM. *A fully automated algorithm for the segmentation of lung fields on digital chest radiographic images*. Medical Physics 1995;22(2):183–191.
- [4] McNitt-Gray MF, Huang HK, Sayre JW. *Feature selection in the pattern classification problem of digital chest radiograph segmentation*. IEEE Transactions on Medical Imaging 1995;14(3):537–547
- [5] S. Hu, E. Hoffman, and J. Reinhardt, "Automatic lung segmentation for accurate quantitation of volumetric x-ray ct images," *Medical Imaging*, IEEE Transactions on, vol. 20, pp. 490–498, June 2001.
- [6] Armato SG, Giger ML, MacMahon H. "Automated lung segmentation in digitized posteroanterior chest radiographs". *Academic Radiology* 1998;5:245–255.

- [7] H. Becker, W. Nettleton, P. Meyers, J. Sweeney, and C. Nice, "Digital computer determination of a medical diagnostic index directly from chest X-ray images," IEEE Trans. Biomed. Eng., vol. 11, pp. 67–72, 1964.
- [8] P. Meyers, C. Nice, H. Becker, W. Nettleton, J. Sweeney, and G. Meckstroth, "Automated computer analysis of radiographic images," Radiology, vol. 83, pp. 1029–1034, 1964.
- [9] A. Mansoor, U. Bagci, Z. Xu, B. Foster, K. N. Olivier, J. M. Elinoff, A. F. Suffredini, J. K. Udupa, and D. J. Mollura, "A generic approach to pathological lung segmentation," IEEE transactions on medical imaging, vol. 33, no. 12, pp. 2293–2310, 2014.
- [10] I. Sluimer, M. Prokop, and B. Van Ginneken, "Toward automated segmentation of the pathological lung in ct," IEEE transactions on medical imaging, vol. 24, no. 8, pp. 1025–1038, 2005.
- [11] E. Hosseini-Asl, J. M. Zurada, and A. El-Baz, "Lung segmentation based on nonnegative matrix factorization," in 2014 IEEE International Conference on Image Processing (ICIP), pp. 877–881, IEEE, 2014.
- [12] Shanhui Sun, Christian Bauer, Reinhard Beichel, "Automated 3-D Segmentation of Lungs With Lung Cancer in CT Data Using a Novel Robust Active Shape Model Approach," IEEE transactions on medical imaging, vol. 31, no. 2, 2012.
- [13] J. Long, E. Shelhamer, and T. Darrell, "Fully convolutional networks for semantic segmentation," in Computer Vision and Pattern Recognition (CVPR 2015), 2015.
- [14] Candemir S., Jaeger S., Palaniappan K. etc. "Lung segmentation in chest radiographs using anatomical atlases with non-rigid registration", IEEE Transactions on Medical Imaging Vol. 33, No. 2, pp. 577–590, 2013
- [15] Jun Lai, Ming Ye, "Active Contour Based Lung Field Segmentation", IEEE International Conference on Intelligent Human-Machine Systems and Cybernetics, pp. 288-291, 2009
- [16] Cai, Yufang & Shen, Kuan & Wang, Jue, "Application of Radon Transform in CT image matching", 2004
- [17] Nwe Nwe Soe, "Image Matching Scheme by using Bhattacharyya Coefficient Algorithm", International Journal of Innovative Research in Computer and Communication Engineering, Vol. 3, Issue 7, July 2015.
- [18] C. Liu, J. Yuen, and A. Torralba, "SIFT Flow: Dense Correspondence across Scenes and its Applications," IEEE Trans. Pattern Analysis and Machine Intelligence, vol. 33, no. 5, pp. 978–994, 2010.
- [19] Sema Candemir, Stefan Jaeger, Kannappan Palaniappan, Sameer Antani, and George Thoma, "Graph Cut Based Automatic Lung Boundary Detection in Chest Radiographs", 1st Annual IEEE Healthcare Innovation Conference, Houston, Texas USA, pp. 7 – 9, 2012
- [20] Y. Boykov and V. Kolmogorov, "An experimental comparison of min-cut/max-flow algorithms for energy minimization in vision", IEEE Transactions on Pattern Analysis and Machine Intelligence, Vol. 26, No. 9, pp. 1124 – 1137, 2004